Supporting Information

The Effect of Hydrofluoroether Cosolvent Addition on Li Solvation in Acetonitrile-Based Solvate Electrolytes and Its Influence on S Reduction in a Li-S battery

Kimberly A. See,[#,±,†] Heng-Liang Wu,[#,±,†] Kah Chun Lau,[±,I] Minjeong Shin,[±,†] Lei Cheng,[±,‡] Mahalingam Balasubramanian,[±,∞] Kevin G. Gallagher, [±,§] Larry A. Curtiss,[±,‡] and Andrew A. Gewirth[*,±,†]

[#] These authors contributed equally to this work.

[±] Joint Center for Energy Storage Research, 9700 S. Cass Avenue, Argonne, IL 60439

[†] Department of Chemistry, University of Illinois at Urbana-Champaign, Urbana, Illinois 61801 United States

[I] Department of Physics and Astronomy, California State University, Northridge, California 91330 United States

[‡] Materials Science Division; [§] Chemical Sciences and Engineering Division; [∞] X-ray Science Division, Advanced Photon Source; Argonne National Laboratory, Argonne, Illinois 60439 United States

Corresponding Author:

*Email: agewirth@illinois.edu

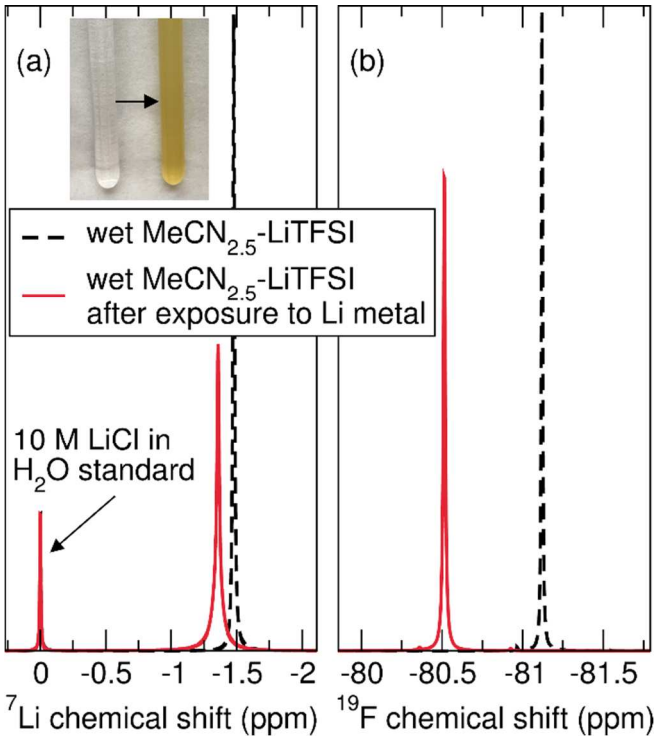

Figure S1. (a) ^{7}Li and (b) ^{19}F NMR of wet $MeCN_{2.5}$–LiTFSI (>50 ppm water) prepared with as-purchased LiTFSI before and after exposure to Li metal. A significant shift in the resonance of both ^{7}Li and ^{19}F is observed after exposure to Li metal due to the decomposition of the electrolyte. A visible color change is observed as shown by the photograph inset in (a). The dry $MeCN_{2.5}$–LiTFSI (<15 ppm water) prepared with dried LiTFSI does not exhibit a color change upon exposure to Li metal.

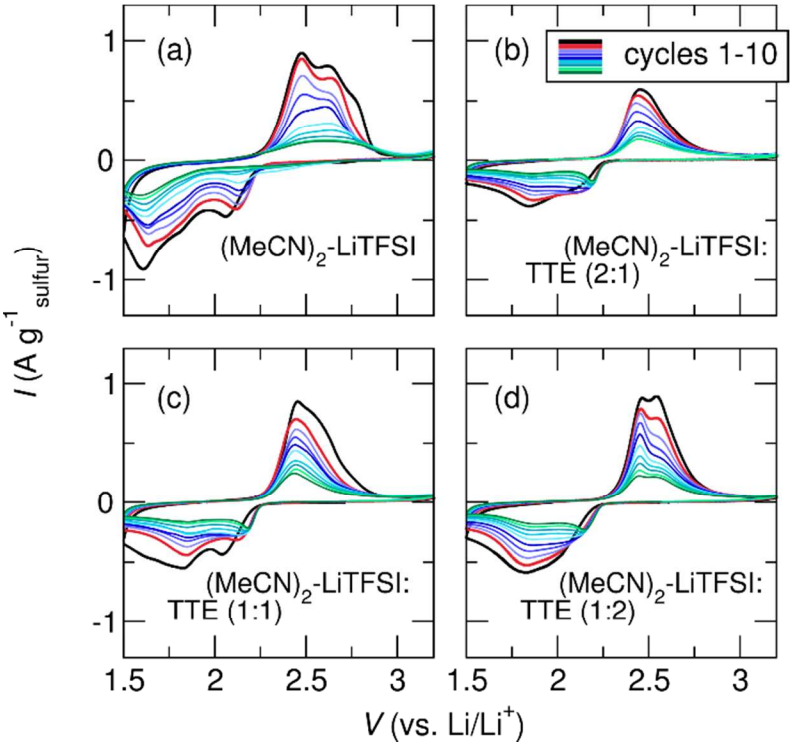

Figure S2. The first 10 cyclic voltammograms (CV) of a Li-S@CMK-3 cells scanned at 0.1 mV s^{-1} with (a) the solvate electrolyte, $(MeCN)_2$–LiTFSI, and the solvate diluted with TTE at volume ratios of (b) 2:1, (c) 1:1, and (d) 1:2 (solvate:TTE).

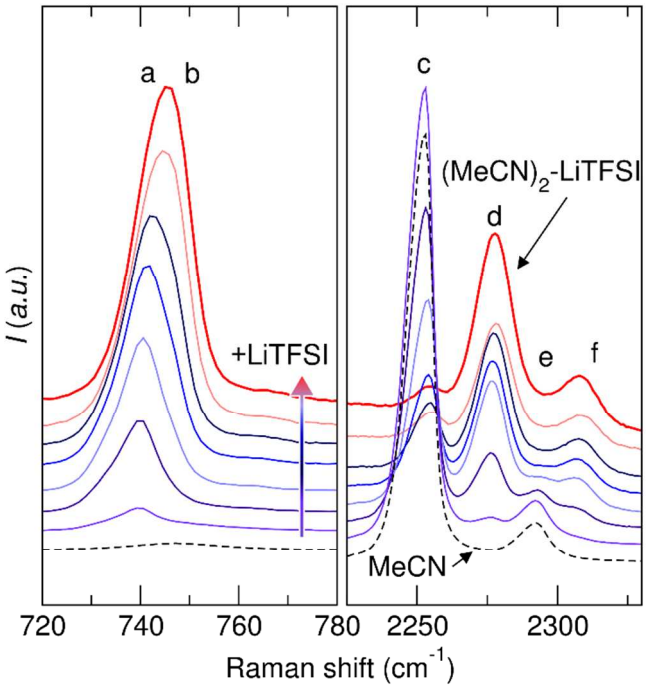

Figure S3. Raman spectra of several concentrations of LiTFSI in MeCN up to the $(MeCN)_2$–LiTFSI at 3.98 M. The concentrations shown are 3.70 M, 2.47 M, 1.85 M, 0.93 M, and 0.46 M. (a) The lower wavenumber region reveals a shift and intensity increase in the TFSI mode, a, to a new mode, mode b, due to coordinated TFSI. (b) The higher wavenumber region shows MeCN modes c, d, e, and f. Modes d and f grow in at the expense of mode c and e, respectively, due to MeCN coordination to Li^+. Mode assignments can be found in Table S1.

Table S1. Assignments of Raman modes in the LiTFSI concentration series in MeCN

	Raman shift (cm^{-1})							Assignment		Ref.
ID	LiTFSI concentration in MeCN (M)							Species	Mode(s)	
	0.46	0.93	1.85	2.47	3.08	3.70	3.98			
a	739	739	740	739	739	739	739	TFSI	S-N stretch + C-S stretch + CF_3 bend	1–4
b	*w*	*w*	*w*	742	744	746	746	TFSI	mode a, coordinated to Li^+	1–4
c	2253	2251	2252	2253	2253	2256	2253	MeCN	C≡N stretch	5,6
d	2276	2276	2276	2276	2277	2278	2278	MeCN	mode c, coordinated to Li^+	7–9
e	2291	2291	2293	2293	2293	2294	2296	MeCN	C–H stretch	5,6
f	i	2305	2308	2306	2307	2308	2308	MeCN	mode e, coordinated to Li^+	

w indicates the mode was either absent or too weak to determine the position.

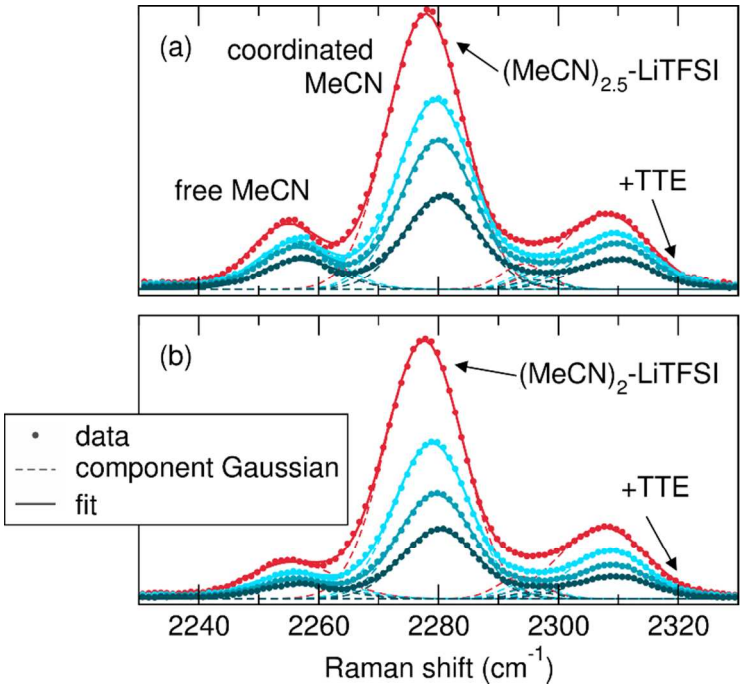

Figure S4. Raman spectra of the (a) $(MeCN)_{2.5}$–LiTFSI and (b) $(MeCN)_2$–LiTFSI neat and diluted with TTE at volume ratios of 2:1, 1:1, and 1:2 (electrolyte:TTE). The spectra is fit with four component Gaussian functions to determine the relative peak area ratios associated with free MeCN and coordinated MeCN.

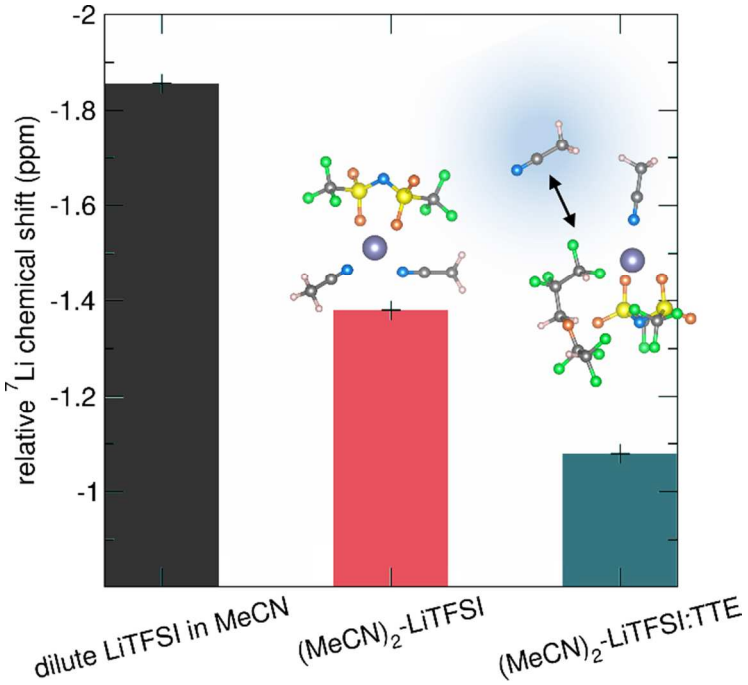

Figure S5. Relative ^{7}Li chemical shifts calculated by DFT for LiTFSI in MeCN in the dilute regime, the $(MeCN)_2$–LiTFSI solvate, and $(MeCN)_2$–LiTFSI diluted with TTE at a volume ratio of 1:1. As the LiTFSI concentration increases from the dilute regime to the $(MeCN)_2$–LiTFSI solvate, the ^{7}Li chemical shift becomes more positive (deshields). Addition of TTE to the $(MeCN)_2$–LiTFSI solvate also causes the ^{7}Li chemical shift to move to a more deshielded region. The shift to more positive ppm as the LiTFSI concentration increases and TTE is added is consistent with the experimental results.

References

(1) Bakker, A.; Gejji, S.; Lindgren, J.; Hermansson, K.; Probst, M. M. *Polymer* **1995**, *36*, 4371–4378.
(2) Edman, L. *J. Phys. Chem. B* **2000**, *104*, 7254–7258.
(3) Herstedt, M.; Smirnov, M.; Johansson, P.; Chami, M.; Grondin, J.; Servant, L.; Lassègues, J. C. *J. Raman Spectrosc.* **2005**, *36*, 762–770.
(4) Brouillette, D.; Irish, D. E.; Taylor, N. J.; Perron, G.; Odziemkowski, M.; Desnoyers, J. E. *Phys. Chem. Chem. Phys.* **2002**, *4*, 6063–6071.
(5) Neelakantan, P. *Proc. Indian Acad. Sci. - Sect. A* **1964**, *60*, 422–424.
(6) Fini, G.; Mirone, P. *Spectrochim. Acta Part Mol. Spectrosc.* **1976**, *32*, 439–440.
(7) Han, S.-D.; Borodin, O.; Seo, D. M.; Zhou, Z.-B.; Henderson, W. A. *J. Electrochem. Soc.* **2014**, *161*, A2042–A2053.
(8) Barthel, J.; Buchner, R.; Wismeth, E. *J. Solut. Chem. 29*, 937–954.
(9) Brouillette, D.; Irish, D. E.; Taylor, N. J.; Perron, G.; Odziemkowski, M.; Desnoyers, J. E. *Phys. Chem. Chem. Phys.* **2002**, *4*, 6063–6071.